

A spectroscopically confirmed Gaia-selected sample of 318 new young stars within ~ 200 pc

Maruša Žerjal,¹ Adam D. Rains,¹ Michael J. Ireland,¹ George Zhou,^{2,3} Jens Kammerer^{1,4}, Alex Wallace¹, Brendan J. Orenstein¹, Thomas Nordlander^{1,5}, Harrison Abbot¹, Seo-Won Chang^{1,6,7,8}

¹Research School of Astronomy & Astrophysics, Australian National University, ACT 2611, Australia

²Center for Astrophysics, Harvard & Smithsonian, 60 Garden St., Cambridge, MA 02138, USA

³Hubble fellow

⁴European Southern Observatory, Karl-Schwarzschild-Str 2, 85748, Garching, Germany

⁵ARC Centre of Excellence for All Sky Astrophysics in 3 Dimensions (ASTRO 3D)

⁶ARC Centre of Excellence for Gravitational Wave Discovery (OzGrav), Australia

⁷SNU Astronomy Research Center, Seoul National University, 1 Gwanak-rho, Gwanak-gu, Seoul 08826, Korea

⁸Astronomy program, Dept. of Physics & Astronomy, Seoul National University, 1 Gwanak-rho, Gwanak-gu, Seoul 08826, Korea

Abstract

While precise parallaxes and proper motions for nearby stars are made available by Gaia, spectroscopic youth indicators for a large fraction of low-mass young stars are still missing. Here we present our observations of 318 new young late K and early M dwarfs within ~ 200 pc that have a detectable lithium line and are not found in the known catalogs of young stars. We also provide measurements of $H\alpha$ and calcium H&K emission and report on additional 126 stars which have no detectable lithium but signs of stellar activity indicating youth. Radial velocities were measured for 756 observed overluminous young star candidates. To infer the origin of these young stars, we are using Chronostar, a novel technique for kinematic characterisation of stellar and their age determination. Our first results in the Scorpius-Centaurus region reveal its complex substructure.

1 Introduction

Young stellar clusters and association are coeval groups of stars comprising a wide range of masses and represent an ideal astrophysical laboratories to study a wide range of phenomena, including star and planetary formation environments. While the adequate cluster membership determination is relatively trivial due to their overdensity with respect to the background, stellar associations representing the vast majority of young stars require more advanced techniques. Accurate parallaxes from the Gaia space telescope (Gaia Collaboration *et al.*, 2018) now for the first time enable a reliable placement of stars in the colour-magnitude diagram and reveal a number of low-mass stars that appear to be overluminous. However, the reasons for their overluminosity besides their youth can be numerous, from the potential multiplicity, the spread due to the different metallicity content to variability in luminosity of young stars. Furthermore, large uncertainties of cool dwarf models due to their strong magnetic fields and inflated radii make the isochronal dating nontrivial. For this reason additional observations of spectroscopic youth indicators are essential to constrain the age of young stars. Here we describe a quest to select and perform a spectroscopic follow-up to measure youth indicators in overluminous stars from the Gaia catalogue on the cool part of the colour-magnitude diagram, as presented in more detail in Žerjal *et al.* (2021).

2 Observations and youth indicators

Our aim was to achieve near-completeness in the survey of youth indicators in the nearby low-mass stars. However, to implement observational constraints and optimise the survey strategy, several cuts were made to the data:

- Colour cut ($3 < BP-W1 < 5.6$) allowed us to focus on stars with the fastest lithium depletion rate, i.e. K5-M3 pre-main sequence dwarfs.
- Luminosity cut takes into account only stars 1 magnitude or more above the main sequence. This approach avoids older main sequence stars and binaries (at most 0.75 magnitude above the main sequence). Additionally, an upper luminosity limit discards giants.
- To avoid the kinematic bias towards young regions and include low-mass stars that can more likely get ejected from the cluster due to gravitational interactions, and at the same time reduce the number of kinematically older stars in the candidate sample, our kinematic cut is very wide. All objects within ($\pm 15, \pm 15, \pm 10$) km s^{-1} of the median UVW = (-11.90, 215.77, 0.19) km s^{-1} are kept in our list. Additionally, the list includes all stars with no radial velocities available.
- Magnitude constraint on the observed Gaia G magnitude ($10 < G < 14.5$) allowed observations with

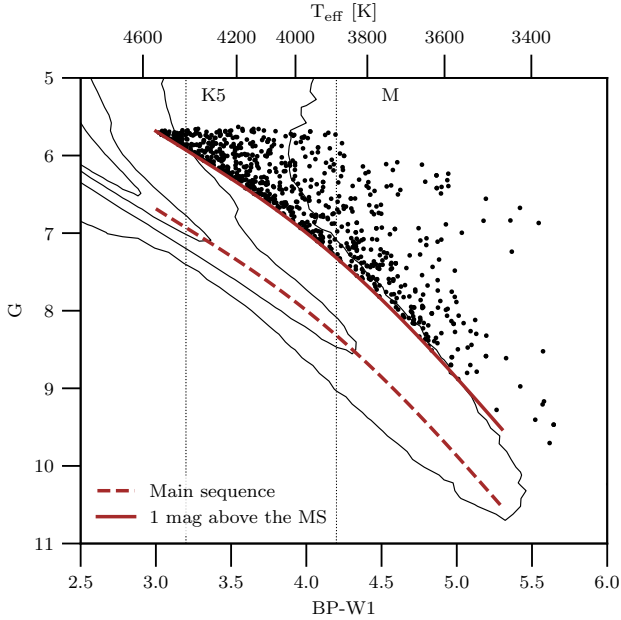


Figure 1: Young star candidates from this work (reddening was not taken into account in this figure). Figure adjusted from Žerjal *et al.* (2021).

the Echelle and WiFeS spectrographs on the ANU 2.3m telescope with reasonable exposure times.

- Declination cut ($\delta < 30$ deg) excluded stars not visible from the Siding Spring Observatory, Australia.

There were no explicit cuts on parallax. To further reduce the sample, known young stars from the Simbad database and young stars from the GALAH survey (Žerjal *et al.*, 2019) were excluded from the list. This selection function resulted in 799 candidate young stars. Their positions in the colour-magnitude diagram is shown in figure 1.

Observations of 756 stars were done with WiFeS (Wide-Field Spectrograph) and Echelle spectrographs on 2.3m ANU telescope in Siding Spring Observatory over 64 nights between November 2018 and October 2019. In particular, 349 stars brighter than $G=12.5$ were observed with slit-fed Echelle spectrograph ($R=24,000$) to achieve better radial velocity precision. Their spectra were reduced with the procedure described in Zhou *et al.* (2014). WiFeS spectrograph (Dopita *et al.*, 2007) with resolving power of 3000 in the blue and 7000 in the red was utilised for stars with $12.5 < G < 14.5$. A standard PyWiFeS package (Childress *et al.*, 2014) was used for the reduction of these spectra.

Computation of radial velocities was based on a template grid of 1D LTE spectra described by Nordlander *et al.* (2019). The precision of the determined radial velocities is 3.2 km s^{-1} for WiFeS spectra and 1.5 km s^{-1} for Echelle spectra. For more details see Žerjal *et al.* (2021).

2.1 Youth indicators

Despite the fact that stellar ages of cool stars on the main sequence are notoriously difficult to determine, several spectroscopic features proved to be useful when constraining age

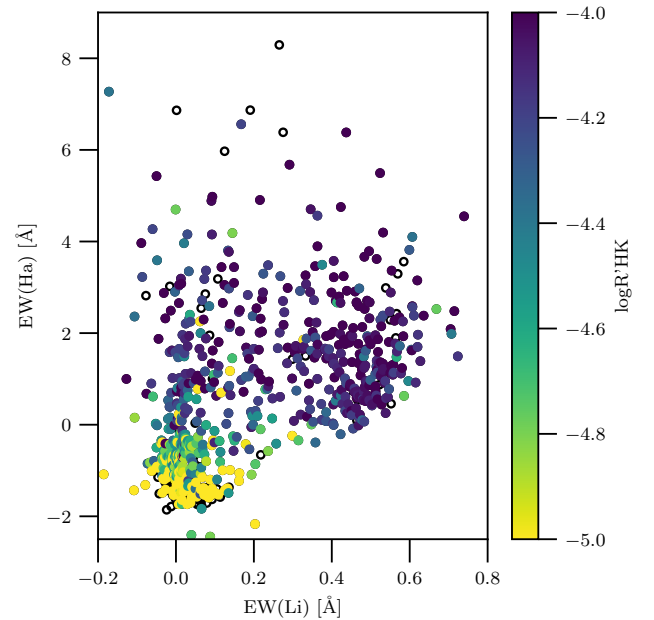


Figure 2: Youth indicators $\log R'_{\text{HK}}$ and $\text{EW}(\text{H}\alpha)$ as proxies for chromospheric activity and $\text{EW}(\text{Li})$ that is an indicator of extreme youth. Figure from Žerjal *et al.* (2021).

of young stars. These youth indicators originate in two different and unrelated phenomena. The first one is chromospheric activity related to the magnetic fields of low-mass stars decaying over time. It is observed as an excess emission in calcium (e.g. Ca II H&K at 3968.47 and 3933.66 Å, respectively) and H α . These indicators typically enable an age estimate with a precision of ~ 0.2 dex between 0.6 and 4.5 Gyr (Mamajek & Hillenbrand, 2008). On the other hand, the destruction of lithium (line at 6708 Å) in the cores of the fully-convective pre-main sequence cool stars on the scales of a few 10 Myr facilitates an upper age limits of these stars.

Our list of measured youth indicators $\log R'_{\text{HK}}$ (a proxy for Ca II H&K), $\text{EW}(\text{H}\alpha)$ and $\text{EW}(\text{Li})$, described in detail in Žerjal *et al.* (2021) and shown in figure 2, confirms a vast number of young stars in the sample. In particular, we found 346 stars showing detectable lithium absorption, 318 of which are not found in the literature. Additionally, we report on 125 stars with detectable signs of stellar activity, but no measurable lithium lines.

Lithium measurements are compared to the lithium isochrones in figure 3. As in Žerjal *et al.* (2019), these isochrones are determined by taking indicative non-LTE equivalent widths from Pavlenko & Magazzu (1996) for Solar metallicity and $\log g = 4.5$ and combining them with the Baraffe *et al.* (2015) models of lithium depletion (assuming the initial absolute abundance of 3.26 from Asplund *et al.*, 2009). The isochrones in figure 3 reveal the extreme youth of a number of stars. Moreover, an overdensity of stars with $\text{EW}(\text{Li}) > 0.4 \text{ \AA}$ indicates a group of stars younger than ~ 10 Myr. We discuss the plan to infer their origin in the next section.

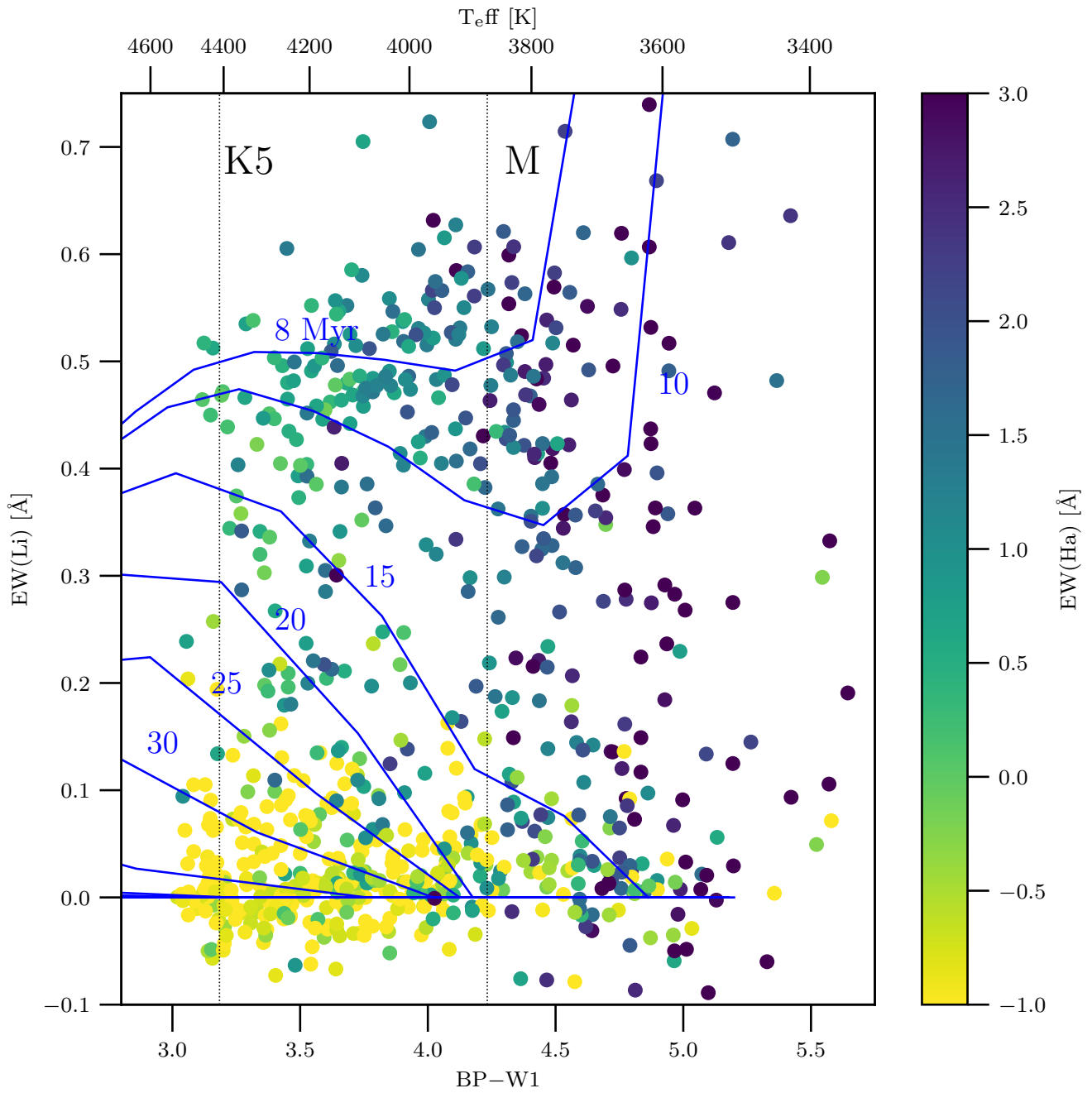


Figure 3: Lithium isochrones help to constrain ages of stars with detectable lithium line. There is an overdensity of stars with ages < 10 Myr. Figure adjusted from Žerjal *et al.* (2021).

3 Stellar associations

Our work provides missing radial velocities and a list of youth indicators for nearby K5-M3 pre-main sequence stars within ~ 200 pc. These measurements complete the set of parameters essential for the investigation of the origin of the low-mass young stars that happen to lie in the direction of the Scorpius-Centaurus association and the Taurus molecular cloud.

The next step in the quest to infer the origin of these young stars is to exploit their kinematics. Chronostar is a new Bayesian tool to determine stellar ages (Crundall *et al.*, 2019). It models a stellar association at its birth location and traces it forward in time to match the present day distribution of its most likely members. Such approach avoids the propagation of observational errors as only the orbit of a model is computed. Another advantage of Chronostar is its use of the Expectation-Maximisation algorithm. It iteratively improves the list of membership probabilities of an association and the fit of an association model to these members. Moreover, it explores the possibility of a multi-component model to better fit the complex sub-densities of an association such as e.g. Scorpius-Centaurus association. Since the majority of the young stars in our sample lie in the direction of the Scorpius-Centaurus association, we selected a 6D cube of stars with known radial velocities from the Gaia DR2 catalogue and performed a fit. Chronostar was able to extract Scorpius-Centaurus members purely from their kinematics and found a 13-component model as the best fit. The preliminary results with most likely members, including stars with missing radial velocities, are shown in figure 4. Their extreme youth is confirmed with the low-mass stars residing above the main sequence.

Acknowledgments

We acknowledge the traditional owners of the land on which the telescope stands, the Gamilaraay people, and pay our respects to elders past and present. This work has made use of data from the European Space Agency (ESA) mission Gaia (<https://www.cosmos.esa.int/gaia>), processed by the Gaia Data Processing and Analysis Consortium (DPAC, <https://www.cosmos.esa.int/web/gaia/dpac/consortium>). Funding for the DPAC has been provided by national institutions, in particular the institutions participating in the Gaia Multilateral Agreement. This publication makes use of data products from the Wide-field Infrared Survey Explorer, which is a joint project of the University of California, Los Angeles, and the Jet Propulsion Laboratory/California Institute of Technology, funded by the National Aeronautics and Space Administration. MŽ acknowledges funding from the Australian Research Council (grant DP170102233). ADR acknowledges support from the Australian Government Research Training Program, and the Research School of Astronomy & Astrophysics top up scholarship. This research made use of Astropy, a community-developed core Python package for Astronomy (Astropy Collaboration 2013, 2018). Parts of this research were supported by the Australian Research Council Centre of Excellence for All Sky Astrophysics in 3 Dimensions (ASTRO 3D), through project number CE170100013. Parts of this research were conducted by the Australian Research Council Centre of Excellence for Gravitational Wave Discovery (OzGrav), through project number CE170100004. S.-W. Chang ac-

knowledges support from the National Research Foundation of Korea (NRF) grant, No. 2020R1A2C3011091, funded by the Korea government (MSIT).

References

- Asplund, M., Grevesse, N., Sauval, A. J., & Scott, P. 2009, *ARA&A*, 47, 481.
- Baraffe, I., Homeier, D., Allard, F., & Chabrier, G. 2015, *A&A*, 577, A42.
- Childress, M. J., Vogt, F. P. A., Nielsen, J., & Sharp, R. G. 2014, *Ap&SS*, 349, 617.
- Crundall, T. D., Ireland, M. J., Krumholz, M. R., Federrath, C., Žerjal, M., *et al.* 2019, *MNRAS*, 489, 3625.
- Dopita, M., Hart, J., McGregor, P., Oates, P., Bloxham, G., *et al.* 2007, *Ap&SS*, 310, 255.
- Gaia Collaboration, Brown, A. G. A., Vallenari, A., Prusti, T., de Bruijne, J. H. J., *et al.* 2018, *A&A*, 616, A1.
- Mamajek, E. E. & Hillenbrand, L. A. 2008, *ApJ*, 687, 1264.
- Nordlander, T., Bessell, M. S., Da Costa, G. S., Mackey, A. D., Asplund, M., *et al.* 2019, *MNRAS*, 488, L109.
- Pavlenko, Y. V. & Magazzu, A. 1996, *A&A*, 311, 961.
- Žerjal, M., Ireland, M. J., Nordlander, T., Lin, J., Buder, S., *et al.* 2019, *MNRAS*, 484, 4591.
- Žerjal, M., Rains, A. D., Ireland, M. J., Zhou, G., Kammerer, J., *et al.* 2021, *MNRAS*, 503, 938.
- Zhou, G., Bayliss, D., Hartman, J. D., Bakos, G. Á., Penev, K., *et al.* 2014, *MNRAS*, 437, 2831.

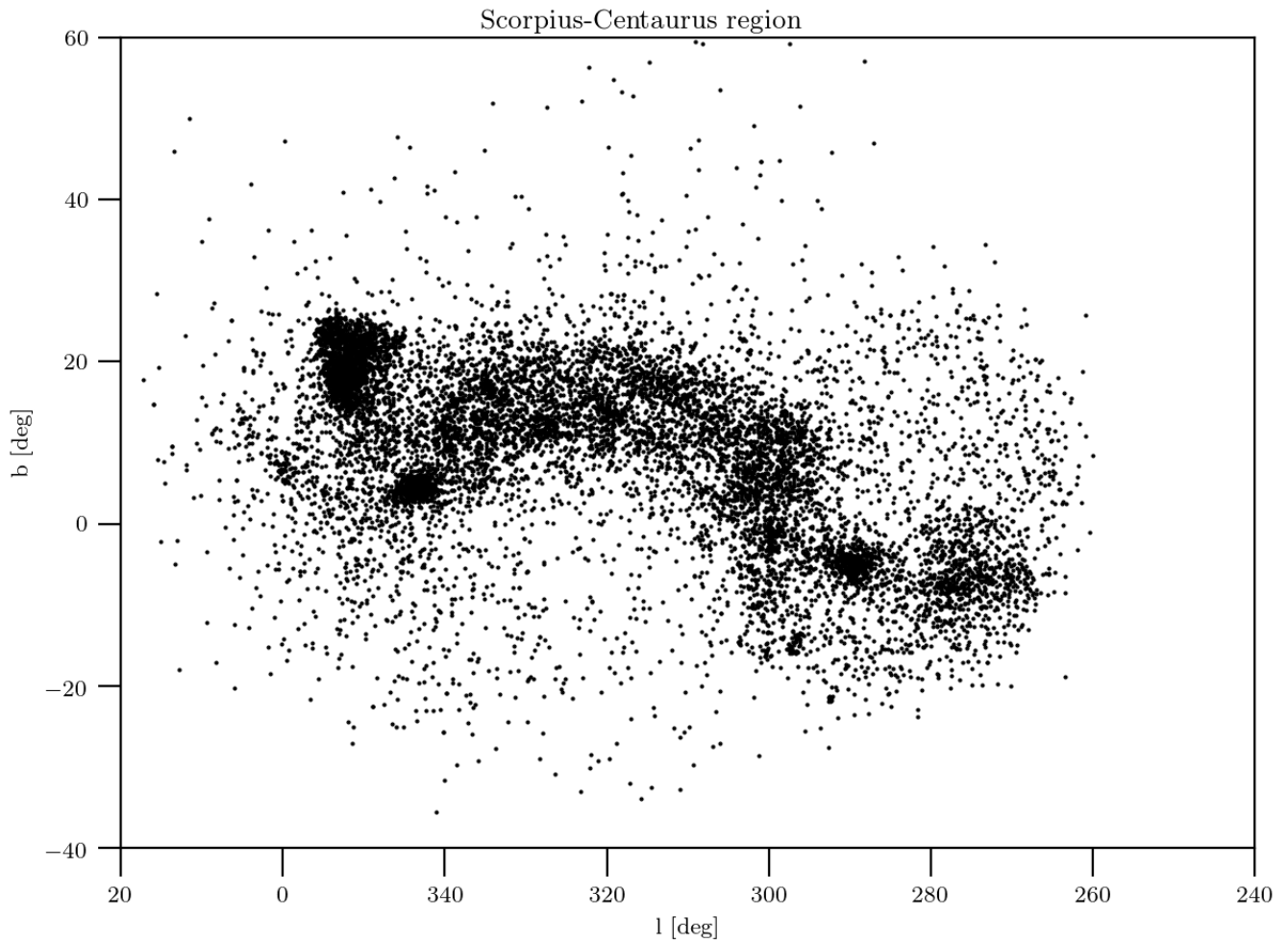


Figure 4: Kinematic components in the Scorpius-Centaurus region as determined with Chronostar. Some components are not shown because they have not converged yet (e.g. component including Corona Australis association), while some other are not associated with this association but appear nearby. These results are preliminary (Žerjal et al., in prep.).